entropy

MDPI

Article

Dark Energy with Phantom Crossing and the H_0 Tension

Eleonora Di Valentino [1,*], Ankan Mukherjee [2,3] and Anjan A. Sen [2,4]

1 Institute for Particle Physics Phenomenology, Department of Physics, Durham University, Durham DH1 3LE, UK
2 Centre for Theoretical Physics, Jamia Millia Islamia, New Delhi 110025, India; ankan.ju@gmail.com (A.M.); aasen@jmi.ac.in (A.A.S.)
3 Department of Physics, Bangabasi College, Kolkata 700009, India
4 School of Arts and Sciences, Ahmedabad University, Ahmedabad 380009, India
* Correspondence: eleonora.di-valentino@durham.ac.uk

Abstract: We investigate the possibility of phantom crossing in the dark energy sector and the solution for the Hubble tension between early and late universe observations. We use robust combinations of different cosmological observations, namely the Cosmic Microwave Background (CMB), local measurement of Hubble constant (H_0), Baryon Acoustic Oscillation (BAO) and SnIa for this purpose. For a combination of CMB+BAO data that is related to early universe physics, phantom crossing in the dark energy sector was confirmed at a 95% confidence level and we obtained the constraint $H_0 = 71.0^{+2.9}_{-3.8}$ km/s/Mpc at a 68% confidence level, which is in perfect agreement with the local measurement by Riess et al. We show that constraints from different combinations of data are consistent with each other and all of them are consistent with phantom crossing in the dark energy sector. For the combination of all data considered, we obtained the constraint $H_0 = 70.25 \pm 0.78$ km/s/Mpc at a 68% confidence level and the phantom crossing happening at the scale factor $a_m = 0.851^{+0.048}_{-0.031}$ at a 68% confidence level.

Keywords: dark energy; cosmic microwave background; Hubble tension

Citation: Di Valentino, E.; Mukherjee, A.; Sen, A.A. Dark Energy with Phantom Crossing and the H_0 Tension. *Entropy* **2021**, *23*, 404. https://doi.org/10.3390/e23040404

Academic Editor: Lino Miramonti and David Kubiznak

Received: 19 February 2021
Accepted: 26 March 2021
Published: 29 March 2021

1. Introduction

The observed phenomenon of cosmic acceleration [1,2] brought revolutionary change in our understanding of the cosmos. To explain the alleged accelerated expansion within the regime of General Relativity, it is essential to introduce some unknown source in the energy budget of the universe. This exotic source of energy is dubbed as *dark energy*. Different prescriptions from different branches of theoretical physics regarding the physical entity of dark energy are available in the literature (see [3] and references therein). The energy density of a vacuum [4–6], scalar fields' energy density [7], or some unknown fluid [8,9] can be candidates for dark energy. However, none of these are beyond ambiguity. The unprecedented technical developments in cosmological observations in the recent years, like the observation of Cosmic Microwave Background (CMB) by Planck [10], the extended Supernova Cosmology Project [11], the observation of baryon distribution in the universe by the Baryon Oscillation Spectroscopic Survey (BOSS) [12], multi-wavelength observation of the large-scale structure of the universe by the Sloan Digital Sky Survey (SDSS) [13], etc., have ensured very precise constraints on cosmological models.

Depending on the nature of the dark energy equation of state, the time varying dark energy models are classified into two sections, namely phantom dark energy ($w_{de} < -1$) and non-phantom dark energy ($w_{de} > -1$). The phantom barrier is delineated by $w_{de} = -1$, which represents the cosmological constant or the vacuum dark energy. The prime motivation of the present work is to check whether cosmological observations allow a dark energy to have a transition from phantom to non-phantom or vice versa. The theoretical background of phantom crossing dark energy are discussed in [14–20], in the composite scalar field model in [21–23], and in the context of Horndeski's Theory [24,25]. Some recent

studies regarding the observational aspects of phantom crossing dark energy are referred to in [26–29]. A recent model independent reconstruction of a dark energy equation state by Zhao et al. [30,31] shows that a combination of cosmological data including CMB data from Planck observations points towards possible phantom crossing in a dark energy equation of state. Similar results have been obtained by Capozziello et al. [32] with only low-redshift data. Moreover, reconstruction procedures for the dark energy density $\rho_{de}(z)$ [29] as well as Hubble parameter $H(z)$ [33] also exhibited phantom crossing in the dark energy sector.

Another serious issue of dark energy reconstruction is the disagreement of the local measurement of the Hubble parameter with the value estimated from the CMB. The local measurements suggest a higher value of the present Hubble parameter (H_0) compared to the value estimated for the standard model composed by a cosmological constant with cold dark matter (ΛCDM) from the CMB likelihood. The latest measurement of H_0, reported by the SH0ES collaboration, is $H_0 = 74.03 \pm 1.42$ km/s/Mpc at a 68% confidence level (CL) [34] and the value estimated by Planck for ΛCDM is $H_0 = 67.27 \pm 0.60$ km/s/Mpc at a 68% CL [35]. The tension is now at a 4.4σ level. There are many attempts to alleviate the issue in the literature (see for an incomplete list of works Refs. [36–78] and the recent overview in [79,80]). It has been recently discussed [81,82] that a transition in absolute magnitude M_B for SnIa can also explain the apparent tension between the local and CMB measurements of the Hubble parameter H_0. Such variation in M_B in SnIa can be related to the apparent variation of the normalized Newtonian constant $\mu = G_{eff}/G_N$.

An important aspect of the present reconstruction is, therefore, to investigate whether a phantom crossing in dark energy evolution can alleviate the present Hubble tension. The present reconstruction is purely phenomenological based on the parametrization of the dark energy density. There is no assumption about the physical entity of dark energy from any theoretical background apart from that it has a phantom crossing at some stage during its evolution. The dark energy density is parametrized using a Taylor series expansion truncated at a certain order. The coefficients of the series expansion are constrained using observational data with a statistical approach. We have assumed that the components in the energy budget, namely the matter, dark energy and radiation, are independently conserved. In the following sections, we discuss the present reconstruction, the observational constraints and finally conclude with overall remarks on the results.

2. Reconstruction of the Model

One can parametrize the phantom crossing behavior in the dark energy either through its equation of state $w_{DE}(z)$ or directly through its energy density $\rho_{DE}(z)$. On the one hand, different observables are directly related to the Hubble parameter $H(z)$ rather than the equation of state of the dark energy fluid. If one parametrizes dark energy with $w_{DE}(z)$, the dark energy contribution in $H(z)$ involves the integration of $w_{DE}(z)$ over the redshift interval, whereas parametrizing dark energy with $\rho_{DE}(z)$ contributes directly to $H(z)$. Hence $\rho_{DE}(z)$ is the simpler and more direct way to parametrize the dark energy contribution in $H(z)$. Hence we chose $\rho_{DE}(z)$ to model the dark energy behavior.

Let us write the energy conservation equation for the dark energy fluid: $\frac{d\rho_{DE}}{da} = -\frac{3}{a}(1 + w_{DE})\rho_{DE}$. It is straightforward to see that for $(1 + w_{DE}) > 0$ (non-phantom models), ρ_{DE} decreases with the scale factor, whereas for $(1 + w_{DE}) < 0$ (phantom models) ρ_{DE} increases with the scale factor. For $w_{DE} = -1$, ρ_{DE} is constant and that is the "Cosmological Constant". Hence, for any phantom crossing, dark energy density should pass through an extremum at some redshift $a = a_m$ where $\frac{d\rho_{DE}}{da}$ changes its sign. We perform a Taylor series expansion of ρ_{DE} around this extremum at $a = a_m$:

$$\begin{aligned}\rho_{DE}(a) &= \rho_0 + \rho_2(a - a_m)^2 + \rho_3(a - a_m)^3 \\ &= \rho_0[1 + \alpha(a - a_m)^2 + \beta(a - a_m)^3].\end{aligned} \tag{1}$$

Here we normalize the present day scale factor $a_0 = 1$. As we have assumed that ρ_{DE} has an extrema at a_m, we have ignored the first order derivative term in the Taylor expansion.

We also restricted ourselves up to the third order in the Taylor expansion. Allowing higher-order terms will involve more parameters in the model that may not be tightly constrained with present data. One should also note that there can be a second extrema in ρ_{DE} depending on the values of α and β. With this, the Hubble parameter can be written as:

$$3H^2 + 3\frac{k}{a^2} = 8\pi G[\rho_m + \rho_\gamma + \rho_{DE}]. \tag{2}$$

Finally we will have:

$$H^2(a)/H_0^2 = \Omega_{m0}a^{-3} + \Omega_{k0}a^{-2} + \Omega_{\gamma 0}a^{-4} + \\ + \left(\frac{1-\Omega_{m0}-\Omega_{k0}-\Omega_{\gamma 0}}{1+\alpha(1-a_m)^2+\beta(1-a_m)^3}\right)\left[1+\alpha(a-a_m)^2+\beta(a-a_m)^3\right], \tag{3}$$

and the dark energy equation of state:

$$w_{DE}(a) = -1 - \frac{a[2\alpha(a-a_m)+3\beta(a-a_m)^2]}{3[1+\alpha(a-a_m)^2+\beta(a-a_m)^3]}. \tag{4}$$

One can easily rewrite the above expression for $w_{DE}(a)$ to show that it represents a Pade series of order (3,3), which has a better convergence radius. Additionally, for early times ($a \to 0$), the equation of state $w_{DE} \to -1$ shows the Cosmological Constant behavior for the dark energy. This confirms that the dark energy equation of state is well behaved at an early time without any convergence issues. It is also not difficult to verify that adding higher-order terms in ρ_{DE} does not change the $w_{DE} \to -1$ behavior at an early time. We should add that the different terms in the expression for ρ_{DE} can be generated by non-canonical scalar fields with Lagrangian $\mathcal{L} \propto -X^{n/(2(3+n))}$ with different values of n, as shown in [83].

A set of model parameters (α, β, a_m) are introduced through the present reconstruction. Clearly the present model mimics the ΛCDM for $\alpha = \beta = 0$. The a_m is the scale factor, where the ρ_{DE} has an extrema. If a_m is constrained to be $a_m < 1$ (we fix $a_0 = 1$ for the present day scale factor), it is a signature of transition in the nature of dark energy. In our subsequent analysis, we assume a spatially flat universe, i.e., $\Omega_{k0} = 0$. We allow the dark energy density ρ_{DE} to become negative, as considered by other works (see for example [29,33,84,85]).

3. Methodology

In order to constrain the Dark Energy models' parameters, we make use of some of the most recent cosmological measurements available. These will be:

- **CMB**: we consider the temperature and polarization CMB angular power spectra of the Planck legacy release of 2018 *plikTTTEEE+lowl+lowE* [35,86] as a baseline (Note that there is an alternative likelihood for the Planck data, CamSpec [87], but they are consistent, as stated clearly from the Planck collaboration).
- **R19**: we adopt the gaussian prior $H_0 = 74.03 \pm 1.42$ km/s/Mpc at a 68% CL on the Hubble constant as measured by the SH0ES collaboration in [34].
- **BAO**: we add the Baryon Acoustic Oscillation (BAO) measurements 6dFGS [88], SDSS MGS [89], and BOSS DR12 [90], as adopted by the Planck collaboration in [35] (Note that there is an updated version of the BAO data [91], but we prefer to keep the combination used in the literature, for a better comparison).
- **Pantheon**: we make use of the luminosity distance data of 1048 type Ia Supernovae from the Pantheon catalog [92].
- **Lensing**: we consider the 2018 CMB lensing reconstruction power spectrum data, obtained with a CMB trispectrum analysis in [93].

We adopt as a baseline a nine-dimensional parameter space, i.e., we vary the following cosmological parameters: the baryon energy density $\Omega_b h^2$, the cold dark matter energy

density $\Omega_c h^2$, the ratio of the sound horizon at decoupling to the angular diameter distance to last scattering θ_{MC}, the optical depth to reionization τ, the amplitude and the spectral index of the primordial scalar perturbations A_s and n_s, and, finally, the three parameters assumed in our expansion of the ρ_{DE} in Equation (1), i.e., α, β and a_m. We impose flat uniform priors on these parameters, as reported in Table 1.

To analyze the data and extract the constraints on these cosmological parameters, we used our modified version of the publicly available Monte Carlo Markov Chain package CosmoMC [94]. This is equipped with a convergence diagnostic based on the Gelman and Rubin statistic [95], assuming $R-1<0.02$, and implements an efficient sampling of the posterior distribution using the fast/slow parameter decorrelations [96]. CosmoMC includes support for the 2018 Planck data release [86] (see http://cosmologist.info/cosmomc/). Finally, since for point $\alpha=\beta=0$, the present model becomes the ΛCDM one, as was already mentioned before, and the likelihood has a singular nature as a_m becomes redundant in this case, we switch back to the unmodified CosmoMC code for the analysis of this point, to avoid problems.

Table 1. Flat priors for the cosmological parameters.

Parameter	Prior
$\Omega_b h^2$	$[0.005, 0.1]$
$\Omega_c h^2$	$[0.005, 0.1]$
τ	$[0.01, 0.8]$
n_s	$[0.8, 1.2]$
$\log[10^{10} A_s]$	$[1.6, 3.9]$
$100\theta_{MC}$	$[0.5, 10]$
α	$[0, 30]$
β	$[0, 30]$
a_m	$[0, 1]$

4. Observational Constraints

In Table 2 we show the constraints at a 68% CL for the cosmological parameters explored in this paper, for different dataset combinations. In Figure 1 we show instead the 2D contour plots and 1D posterior distribution on some of the most interesting parameters. We are not showing the CMB-only constraints because they are bimodal in a_m, i.e., CMB alone is not able to distinguish which is its best value in fitting the data, but we need additional probes to break the degeneracy. Eventually, we found that CMB+lensing prefers one of the two peaks, while all the other combinations (+BAO, +Pantheon and +R19) prefer the other peak (see Figure 2). Finally, in Table 3 we compare the χ^2_{bf} of the best fit of the data for the standard ΛCDM model and the phantom crossing. We can see that in all the combinations of data considered here, the phantom crossing model improved the $\Delta\chi^2$ with respect to the standard model.

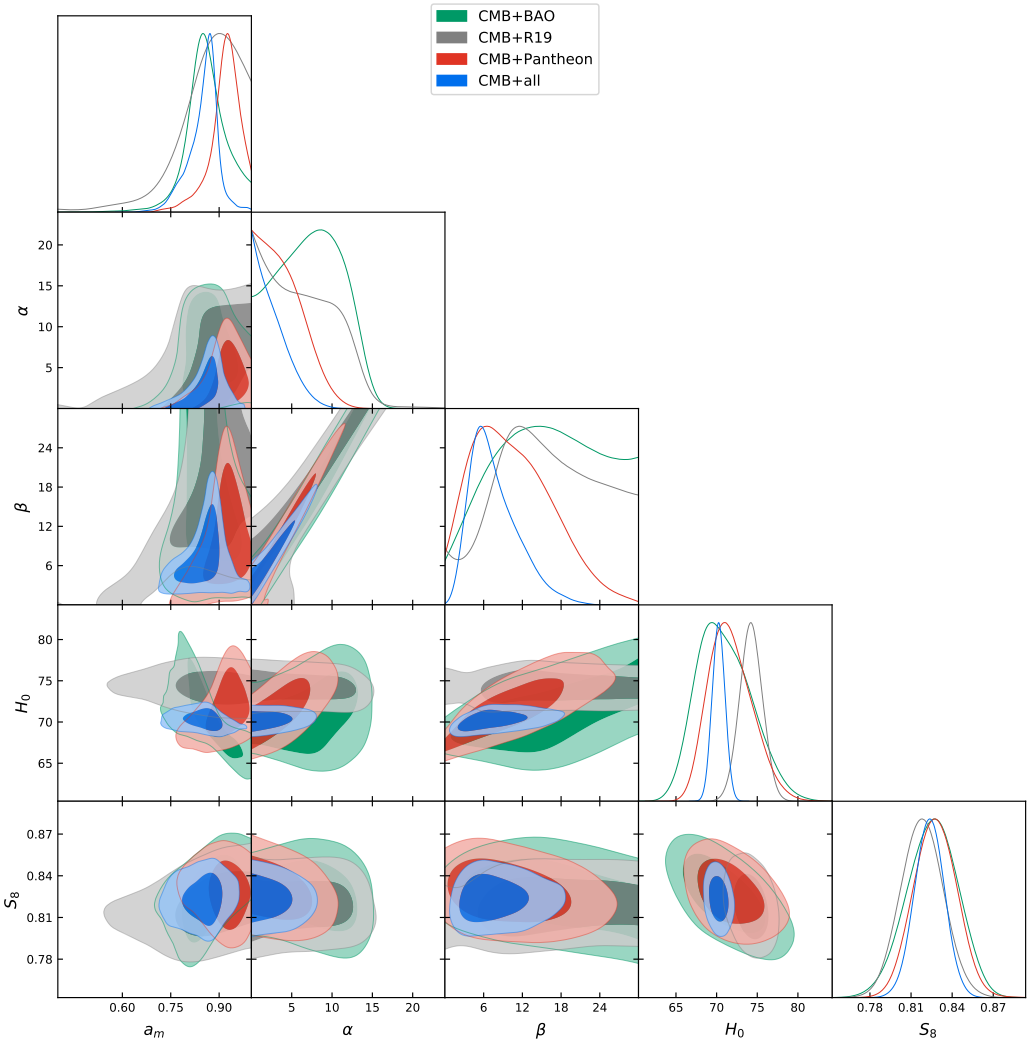

Figure 1. Triangular plot showing 2D and 1D posterior distributions of some interesting parameters considered in this work. Planck+all refers to Planck+lensing+BAO+R19+Pantheon. CMB: Cosmic Microwave Background; BAO: Baryon Acoustic Oscillation.

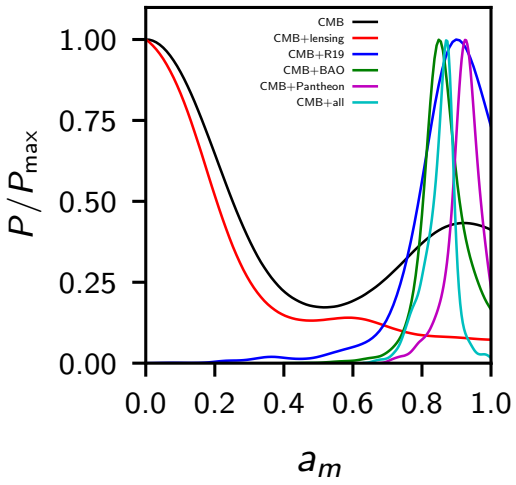

Figure 2. 1D posterior distribution of a_m for the different dataset combinations explored in this work. CMB+all refers to Planck+lensing+BAO+R19+Pantheon.

Comparing the constraints on the cosmological parameters reported in Table 2 for our scenario with those reported by the Planck collaboration in [35] for a wCDM model, we can see that they are completely in agreement for the CMB+lensing dataset combination (second column). This happens because the scale factor of the transition a_m is consistent with zero, so in agreement with a phantom dark energy as preferred by Planck in the wCDM model. Moreover, both α and β are consistent with 0, i.e., a cosmological constant, within one standard deviation. For CMB+lensing we found that the Hubble constant parameter is almost unconstrained ($H_0 > 75.4$ km/s/Mpc at a 95% CL), and $S_8 = 0.752^{+0.009}_{-0.025}$ at a 68% CL is completely in agreement within one standard deviation with the combination of the cosmic shear data KiDS+VIKING-450+DES-Y1 [97], whereas the tension on S_8 is at 3.2σ in a ΛCDM context.

Since the CMB and R19 are in agreement now within two standard deviations, we can combine them safely together. The results we obtained for the joint analysis CMB+R19 are reported in the third column of Table 2. Here we see that while α is still consistent with zero within 1σ, we now have $\beta = 16.0 \pm 7.5$ at a 68% CL and $a_m > 0.830$ at a 68% CL, i.e., consistent with 1.

An interesting result is the one obtained combining CMB and BAO together, which is shown in the forth column of Table 2. Here we can see that contrary to many other cosmological scenarios, including a ΛCDM model of which our parametrization is an extension, CMB+BAO gave $H_0 = 71.0^{+2.9}_{-3.8}$ km/s/Mpc at a 68% CL. This large Hubble constant value is now perfectly consistent within one standard deviation with the R19 measurement, while all other cosmological parameters are almost unchanged if compared with a wCDM scenario for the same CMB+BAO data combination. This increase of the H_0 parameter is due to its positive correlation with α and β, and negative correlation with a_m, as can be seen in Figure 1. For the CMB+BAO case we have in fact an indication that all these three parameters are different from the expected values at more than 1σ. In particular we find, at a 68% CL, $a_m = 0.859 \pm 0.064$, $\alpha = 7.3 \pm 3.9$ and $\beta = 16.1 \pm 7.8$. Therefore, in this case there is an indication at more than 2σ for a transition in the dark energy density. The constraint on the present day equation of state $w_{DE}(z = 0)$ is $-1.61^{+0.60}_{-0.91}$ at a 95% CL, ruling out the cosmological constant at about 2σ. Given that both CMB and BAO are related to early universe physics, this shows that a phantom crossing in dark energy sectors alleviates the tension between the early and late universe determinations of the parameter H_0. In the left panel of Figure 3, we show the behavior of the expansion rate of the universe for this dataset combination. We can see an excellent agreement with all the latest measurements. This agreement finds confirmation in the χ^2_{bf} (see Table 3), where we show that the phantom crossing model improved the $\Delta\chi^2$ with respect to the standard ΛCDM model, not only for the Planck+BAO combination, but also for the BAO data alone.

The same interesting larger value of the Hubble constant persists even if we combine CMB and Pantheon data. In this case, as we show in the fifth column of Table 2, $H_0 = 71.7^{+2.2}_{-3.1}$ km/s/Mpc at a 68% CL, i.e., consistent with R19. As can be seen in Figure 1, it is the positive correlation between H_0 and α and β that shifts the Hubble constant towards higher values, whereas, on the contrary with respect to the CMB+BAO combination, in this case there is a positive correlation also between H_0 and a_m. For the dark energy parameters of our model we found for CMB+Pantheon, at a 68% CL, $a_m = 0.917^{+0.054}_{-0.029}$ and $\beta = 10.6^{+4.4}_{-7.9}$, i.e., different from the expected value in a ΛCDM model at more than 1σ, while $\alpha < 5.10$ is consistent with zero.

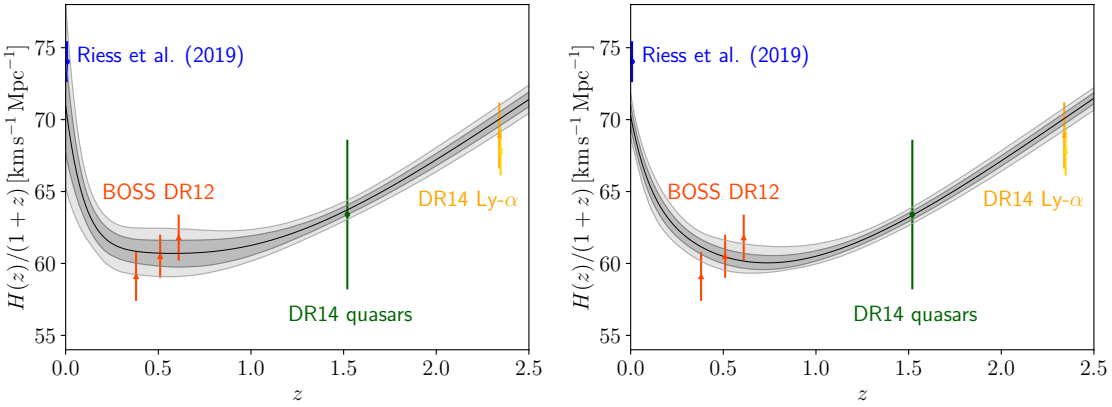

Figure 3. Behavior of $H(z)/(1+z)$ for the combinations CMB+BAO (on the **left**) and CMB+all (on the **right**). Observational data points of local measurement of H_0 by Riess et al. [34], BOSS DR12 [90], BOSS DR14 quasars [98], and BOSS DR14 Ly-α [99,100] are also shown.

Given a preference for all data combinations of a large H_0, we can conclude that this indication is robust irrespective to the combination of data analyzed here. For this reason we combine them all together because they are no more in tension. In fact, even the Planck+lensing dataset combination resulted in $H_0 > 75.4$ km/s/Mpc at a 95% CL, i.e., in perfect agreement with R19. The joint result, i.e., CMB+lensing+BAO+Pantheon+R19, is displayed in the last column of Table 2, where we see $H_0 = 70.25 \pm 0.78$ km/s/Mpc at a 68% CL, reducing the tension with R19 at 2.3 standard deviations. In the right panel of Figure 3, we show the behavior of the expansion rate of the universe for this combination. Also in this case, we can see a good agreement with all of the latest measurements of BAO. However, even if for this dataset combination we have a slightly lower $S_8 = 0.823 \pm 0.011$ at a 68% CL, the tension with the cosmic shear data KiDS+VIKING-450+DES-Y1 [97] is still at 3.1σ. For the joint case we found, at a 68% CL, $a_m = 0.851^{+0.048}_{-0.031}$ and $\beta = 7.7^{+2.2}_{-4.7}$, i.e., they are different from the expected value in a ΛCDM scenario at more than 2σ because they are highly non-gaussian, while $\alpha < 3.32$ at a 68% CL is consistent with zero. Therefore, a robust indication at more than 2σ for a transition in the dark energy density is suggested by the data. The constraint on the present day equation of state $w_{DE}(z=0)$ is $-1.33^{+0.31}_{-0.42}$ at a 95% CL, ruling out the cosmological constant at more than 2σ. Finally, if we look at the χ^2_{bf} in Table 3, we can see that the Phantom Crossing model improves significantly the total $\Delta\chi^2$ we had for the standard ΛCDM model.

From the constraints on r_d in Table 3 for different data combinations, especially for the CMB+BAO combination, we can say that our results agree with BAO data, as well as a larger H_0 value, even if we do not change r_d as constrained by Planck for ΛCDM. This may be due to non-monotonic dark energy evolution in late time.

It is also not difficult to check that $\rho_{DE}(z)$ for the constrained parameter space can become negative for some redshifts and this is consistent with earlier results by [29,33,84,85]. A negative $\rho_{DE}(z)$ at some earlier time may help reduce the Hubble tension.

Additionally, to perform a model comparison, we computed the Bayesian evidence and we show the results in Table 4. This allowed us to quantify which model fits the data better between ΛCDM and phantom crossing. We used the publicly available cosmological code `MCEvidence` (https://github.com/yabebalFantaye/MCEvidence [101,102]). We assumed that for negative (positive) values of the Bayes factor $\ln B_{ij}$, the ΛCDM (phantom crossing) is the preferred model. To interpret the results, we referred to the revised Jeffreys scale by Kass and Raftery as in Reference [103]. Therefore, we will have for $0 \leq |\ln B_{ij}| < 1$ weak evidence, for $1 \leq |\ln B_{ij}| < 3$ definite evidence, for $3 \leq |\ln B_{ij}| < 5$ strong evidence, and for $|\ln B_{ij}| \geq 5$ very strong evidence for one model versus the second one. Looking at Table 4 we can see that we have very strong evidence for the phantom crossing for CMB+R19, while the ΛCDM model is preferred for all other dataset combinations.

Table 2. 68% confidence level (CL) constraints on the cosmological parameters for the different dataset combinations explored in this work. CMB+all refers to Planck+lensing+BAO+R19+Pantheon.

Parameters	CMB+Lensing	CMB+R19	CMB+BAO	CMB+Pantheon	CMB+All
a_m	< 0.276	> 0.830	0.859 ± 0.064	$0.917^{+0.054}_{-0.029}$	$0.851^{+0.048}_{-0.031}$
α	< 17.7	< 8.62	7.3 ± 3.9	< 5.10	< 3.32
β	< 16.7	16.0 ± 7.5	16.1 ± 7.8	$10.6^{+4.4}_{-7.9}$	$7.7^{+2.2}_{-4.7}$
$\Omega_c h^2$	0.1194 ± 0.0014	0.1196 ± 0.0014	0.1201 ± 0.0013	0.1198 ± 0.0014	0.1198 ± 0.0011
$\Omega_b h^2$	0.02243 ± 0.00014	0.02243 ± 0.00016	0.02238 ± 0.00014	0.02240 ± 0.00015	0.02240 ± 0.00014
$100\theta_{MC}$	1.04097 ± 0.00031	1.04096 ± 0.00032	1.04092 ± 0.00030	1.04095 ± 0.00032	1.04093 ± 0.00030
τ	0.0521 ± 0.0076	0.0532 ± 0.0080	$0.0539^{+0.0070}_{-0.0080}$	0.0529 ± 0.0076	0.0521 ± 0.0075
n_s	0.9667 ± 0.0042	0.9665 ± 0.0045	0.9652 ± 0.0043	0.9659 ± 0.0045	0.9655 ± 0.0038
$\ln(10^{10} A_s)$	3.038 ± 0.015	3.041 ± 0.016	3.044 ± 0.016	3.041 ± 0.016	3.039 ± 0.015
$H_0[\mathrm{km/s/Mpc}]$	> 92.8	74.2 ± 1.4	$71.0^{+2.9}_{-3.8}$	$71.7^{+2.2}_{-3.1}$	70.25 ± 0.78
σ_8	$1.012^{+0.051}_{-0.009}$	0.881 ± 0.018	$0.848^{+0.027}_{-0.034}$	$0.860^{+0.026}_{-0.033}$	0.838 ± 0.011
S_8	$0.752^{+0.009}_{-0.025}$	0.818 ± 0.016	0.826 ± 0.019	0.828 ± 0.016	0.823 ± 0.011
r_{drag}	$147.19^{+0.28}_{-0.26}$	147.14 ± 0.30	147.06 ± 0.29	147.10 ± 0.30	147.10 ± 0.25

Table 3. χ^2_{bf}s comparison between ΛCDM and Phantom Crossing for the different dataset combinations explored in this work. CMB+all refers to Planck+lensing+BAO+R19+Pantheon.

ΛCDM	CMB+Lensing	CMB+R19	CMB+BAO	CMB+Pantheon	CMB+All
$\chi^2_{bf,\mathrm{tot}}$	2782.040	2791.838	2779.712	3807.500	3840.406
$\chi^2_{bf,\mathrm{CMB}}$	2778.122	2768.113	2770.060	2767.697	2779.508
$\chi^2_{bf,\mathrm{lensing}}$	8.981	–	–	–	9.510
$\chi^2_{bf,\mathrm{R19}}$	–	18.117	–	–	16.414
$\chi^2_{bf,\mathrm{BAO}}$	–	–	6.514	–	5.271
$\chi^2_{bf,\mathrm{Pantheon}}$	–	–	–	1035.268	1034.768
Phantom Crossing	**CMB+Lensing**	**CMB+R19**	**CMB+BAO**	**CMB+Pantheon**	**CMB+All**
$\chi^2_{bf,\mathrm{tot}}$	2776.610	2765.556	2775.204	3805.278	3828.424
$\chi^2_{bf,\mathrm{CMB}}$	2770.124	2762.965	2763.945	2765.943	2775.585
$\chi^2_{bf,\mathrm{lensing}}$	8.145	–	–	–	8.702
$\chi^2_{bf,\mathrm{R19}}$	–	0.307	–	–	8.275
$\chi^2_{bf,\mathrm{BAO}}$	–	–	5.321	–	5.702
$\chi^2_{bf,\mathrm{Pantheon}}$	–	–	–	1036.603	1035.971

Table 4. The table shows the values of $\ln B_{ij}$ calculated for the phantom crossing model with respect to the ΛCDM scenario. The negative value in $\ln B_{ij}$ indicates that there is a preference for ΛCDM against the phantom crossing model, while a positive value indicates a preference for phantom crossing.

Data	$\ln B_{ij}$
CMB	0.30
CMB+lensing	0.13
CMB+R19	6.91
CMB+BAO	−2.29
CMB+Pantheon	−4.46
CMB+all	−1.75

5. Conclusions

In this work, we considered a dark energy behavior with phantom crossing and confronted it with different observational data including the latest CMB data from Planck. We did not consider any specific theoretical setup involving fields but rather we approached

it in a general way where we assumed that the dark energy density should have an extrema at a particular scale factor a_m for phantom crossing. If $a_m < 1$, this crossing happens before the present day. We Taylor expanded the dark energy density around this extrema and checked whether the observational data are consistent with $a_m < 1$. We found that a combination of observational data including that from Planck is indeed consistent with $a_m < 1$, confirming the presence of phantom crossing. Moreover, the phantom crossing also helps to alleviate the H_0 tension between low and high redshift observations. The CMB+BAO combination, which represents early universe physics, gave the constraint $H_0 = 71.0^{+2.9}_{-3.8}$ km/s/Mpc at a 68% CL for the model with phantom crossing, which is fully in agreement with the local measurement of H_0 by R19. Moreover, constraints on different parameters including H_0 for different combinations of data were found to be consistent with each other, which allowed us to combine all the data. For the combination of all data, the phantom crossing was observed at more than 2σ and the constraint on H_0 was $H_0 = 70.25 \pm 0.78$ km/s/Mpc at a 68% CL, which is in tension with R19 at 2.3 standard deviations—much lower than the present tension with ΛCDM and many other dark energy models, suggesting a substantial alleviation of the Hubble tension with phantom crossing. Finally, as seen in Table 3, the phantom crossing model fit better than ΛCDM the full dataset combination, improving the χ^2_{bf}.

Author Contributions: Conceptualization, A.M. and A.A.S.; methodology, E.D.V.; formal analysis, E.D.V.; writing—original draft preparation, E.D.V., A.M. and A.A.S.; writing—review and editing, E.D.V., A.M. and A.A.S. All authors have read and agreed to the published version of the manuscript.

Funding: E.D.V. acknowledges the support of the Addison–Wheeler Fellowship awarded by the Institute of Advanced Study at Durham University. A.M. acknowledges the financial support from the Science and Engineering Research Board (SERB), Department of Science and Technology, Government of India as a National Post-Doctoral Fellow (NPDF, File no. PDF/2018/001859). A.A.S. acknowledges funding from DST-SERB, Govt. of India, under the project NO. MTR/2019/000599. The authors also thank Ruchika for computational help.

Data Availability Statement: All the datasets used are publicly available and a description can be found in the methodology section.

Conflicts of Interest: The authors declare no conflict of interest.

References

1. Riess, A.G.; Filippenko, A.V.; Challis, P.; Clocchiatti, A.; Diercks, A.; Garnavich, P.M.; Gilliland, R.L.; Hogan, C.J.; Jha, S.; Kirshner, R.P. Observational evidence from supernovae for an accelerating universe and a cosmological constant. *Astron. J.* **1998**, *116*, 1009. [CrossRef]
2. Perlmutter, S.; Aldering, G.; Goldhaber, G.; Knop, R.; Nugent, P.; Castro, P.G.; Deustua, S.; Fabbro, S.; Goobar, A.; Groom, D.E. Measurements of Ω and Λ from 42 high redshift supernovae. *Astrophys. J.* **1999**, *517*, 565. [CrossRef]
3. Bamba, K.; Capozziello, S.; Nojiri, S.I.; Odintsov, S.D. Dark energy cosmology: The equivalent description via different theoretical models and cosmography tests. *Astrophys. Space Sci.* **2012**, *342*, 155–228. [CrossRef]
4. Carroll, S.M. The cosmological constant. *Living Rev. Rel.* **2001**, *4*, 1–56. [CrossRef]
5. Peebles, P.J.E.; Ratra, B. The cosmological constant and dark energy. *Rev. Mod. Phys.* **2003**, *75*, 559. [CrossRef]
6. Padmanabhan, T. Cosmological constant—the weight of the vacuum. *Phys. Rep.* **2003**, *380*, 235–320. [CrossRef]
7. Copeland, E.J.; Sami, M.; Tsujikawa, S. Dynamics of dark energy. *Int. J. Mod. Phys. D* **2006**, *15*, 1753–1935. [CrossRef]
8. Kamenshchik, A.; Moschella, U.; Pasquier, V. An alternative to quintessence. *Phys. Lett. B* **2001**, *511*, 265–268. [CrossRef]
9. Bento, M.; Bertolami, O.; Sen, A.A. Generalized Chaplygin gas, accelerated expansion, and dark-energy-matter unification. *Phys. Rev. D* **2002**, *66*, 043507. [CrossRef]
10. Akrami, Y.; Arroja, F.; Ashdown, M.; Aumont, J.; Baccigalupi, C.; Ballardini, M.; Banday, A.; Barreiro, R.; Bartolo, N.; Basak, S. Planck 2018 results. I. Overview and the cosmological legacy of Planck. *arXiv* **2018**, arXiv:1807.06205.
11. Suzuki, N.; Rubin, D.; Lidman, C.; Aldering, G.; Amanullah, R.; Barbary, K.; Barrientos, L.; Botyanszki, J.; Brodwin, M.; Connolly, N. The Hubble Space Telescope cluster supernova survey. V. Improving the dark-energy constraints above z> 1 and building an early-type-hosted supernova sample. *Astrophys. J.* **2012**, *746*, 85. [CrossRef]
12. Dawson, K.S.; Schlegel, D.J.; Ahn, C.P.; Anderson, S.F.; Aubourg, É.; Bailey, S.; Barkhouser, R.H.; Bautista, J.E.; Beifiori, A.; Berlind, A.A. The Baryon oscillation spectroscopic survey of SDSS-III. *Astron. J.* **2012**, *145*, 10. [CrossRef]

13. Alam, S.; Albareti, F.D.; Prieto, C.A.; Anders, F.; Anderson, S.F.; Anderton, T.; Andrews, B.H.; Armengaud, E.; Aubourg, É.; Bailey, S. The eleventh and twelfth data releases of the Sloan Digital Sky Survey: Final data from SDSS-III. *Astrophys. J. Suppl. Ser.* **2015**, *219*, 12. [CrossRef]
14. Vikman, A. Can dark energy evolve to the phantom? *Phys. Rev. D* **2005**, *71*, 023515. [CrossRef]
15. Nojiri, S.I.; Odintsov, S.D. Inhomogeneous equation of state of the universe: Phantom era, future singularity, and crossing the phantom barrier. *Phys. Rev. D* **2005**, *72*, 023003. [CrossRef]
16. Nojiri, S.I.; Odintsov, S.D. Unifying phantom inflation with late-time acceleration: Scalar phantom–non-phantom transition model and generalized holographic dark energy. *Gen. Relativ. Gravit.* **2006**, *38*, 1285–1304. [CrossRef]
17. Nojiri, S.I.; Odintsov, S.D. The oscillating dark energy: Future singularity and coincidence problem. *Phys. Lett. B* **2006**, *637*, 139–148. [CrossRef]
18. Bamba, K.; Geng, C.-Q.; Nojiri, S.I.; Odintsov, S.D. Crossing of the phantom divide in modified gravity. *Phys. Rev. D* **2009**, *79*, 083014. [CrossRef]
19. Jaime, L.G.; Jaber, M.; Escamilla-Rivera, C. New parametrized equation of state for dark energy surveys. *Phys. Rev. D* **2018**, *98*, 083530. [CrossRef]
20. Saridakis, E.N. Phantom crossing and quintessence limit in extended nonlinear massive gravity. *Class. Quantum Gravity* **2013**, *30*, 075003. [CrossRef]
21. Chimento, L.P.; Forte, M.; Lazkoz, R.; Richarte, M.G. Internal space structure generalization of the quintom cosmological scenario. *Phys. Rev. D* **2009**, *79*, 043502. [CrossRef]
22. Hu, W. Crossing the phantom divide: Dark energy internal degrees of freedom. *Phys. Rev. D* **2005**, *71*, 047301. [CrossRef]
23. Wei, H.; Cai, R.-G. A note on crossing the phantom divide in hybrid dark energy model. *Phys. Lett. B* **2006**, *634*, 9–13. [CrossRef]
24. Deffayet, C.; Pujolas, O.; Sawicki, I.; Vikman, A. Imperfect dark energy from kinetic gravity braiding. *J. Cosmol. Astropart. Phys.* **2010**, *2010*, 026. [CrossRef]
25. Matsumoto, J. Phantom crossing dark energy in Horndeski's theory. *Phys. Rev. D* **2018**, *97*, 123538. [CrossRef]
26. Nesseris, S.; Perivolaropoulos, L. Crossing the phantom divide: Theoretical implications and observational status. *J. Cosmol. Astropart. Phys.* **2007**, *2007*, 018. [CrossRef]
27. Fang, W.; Hu, W.; Lewis, A. Crossing the phantom divide with parametrized post-Friedmann dark energy. *Phys. Rev. D* **2008**, *78*, 087303. [CrossRef]
28. Shafer, D.L.; Huterer, D. Chasing the phantom: A closer look at Type Ia supernovae and the dark energy equation of state. *Phys. Rev. D* **2014**, *89*, 063510. [CrossRef]
29. Wang, Y.; Pogosian, L.; Zhao, G.-B.; Zucca, A. Evolution of dark energy reconstructed from the latest observations. *Astrophys. J. Lett.* **2018**, *869*, L8. [CrossRef]
30. Zhao, G.-B.; Crittenden, R.G.; Pogosian, L.; Zhang, X. Examining the evidence for dynamical dark energy. *Phys. Rev. Lett.* **2012**, *109*, 171301. [CrossRef]
31. Zhao, G.-B.; Raveri, M.; Pogosian, L.; Wang, Y.; Crittenden, R.G.; Handley, W.J.; Percival, W.J.; Beutler, F.; Brinkmann, J.; Chuang, C.-H. Dynamical dark energy in light of the latest observations. *Nat. Astron.* **2017**, *1*, 627–632. [CrossRef]
32. Capozziello, S.; Sen, A.A. Model-independent constraints on dark energy evolution from low-redshift observations. *Mon. Not. R. Astron. Soc.* **2019**, *484*, 4484–4494. [CrossRef]
33. Dutta, K.; Roy, A.; Sen, A.A.; Sheikh-Jabbari, M. Beyond ΛCDM with low and high redshift data: Implications for dark energy. *Gen. Relativ. Gravit.* **2020**, *52*, 1–16. [CrossRef]
34. Riess, A.G.; Casertano, S.; Yuan, W.; Macri, L.M.; Scolnic, D. Large Magellanic Cloud Cepheid standards provide a 1% foundation for the determination of the Hubble constant and stronger evidence for physics beyond ΛCDM. *Astrophys. J.* **2019**, *876*, 85. [CrossRef]
35. Aghanim, N.; Akrami, Y.; Ashdown, M.; Aumont, J.; Baccigalupi, C.; Ballardini, M.; Banday, A.; Barreiro, R.; Bartolo, N.; Basak, S. Planck 2018 results-VI. Cosmological parameters. *Astron. Astrophys.* **2020**, *641*, A6.
36. Di Valentino, E.; Melchiorri, A.; Silk, J. Reconciling Planck with the local value of H0 in extended parameter space. *Phys. Lett. B 2016*, *761*, 242–246. [CrossRef]
37. Bernal, J.L.; Verde, L.; Riess, A.G. The trouble with H0. *J. Cosmol. Astropart. Phys.* **2016**, *2016*, 019. [CrossRef]
38. Kumar, S.; Nunes, R.C. Probing the interaction between dark matter and dark energy in the presence of massive neutrinos. *Phys. Rev. D* **2016**, *94*, 123511. [CrossRef]
39. Kumar, S.; Nunes, R.C. Echo of interactions in the dark sector. *Phys. Rev. D* **2017**, *96*, 103511. [CrossRef]
40. Di Valentino, E.; Melchiorri, A.; Mena, O. Can interacting dark energy solve the H 0 tension? *Phys. Rev. D* **2017**, *96*, 043503. [CrossRef]
41. Di Valentino, E.; Bœhm, C.; Hivon, E.; Bouchet, F.R. Reducing the H_0 and σ_8 tensions with Dark Matter-neutrino interactions. *Phys. Rev. D* **2018**, *97*, 043513. [CrossRef]
42. Di Valentino, E.; Linder, E.V.; Melchiorri, A. Vacuum phase transition solves the H_0 tension. *Phys. Rev. D* **2018**, *97*, 043528. [CrossRef]
43. Di Valentino, E.; Melchiorri, A.; Linder, E.V.; Silk, J. Constraining dark energy dynamics in extended parameter space. *Phys. Rev. D* **2017**, *96*, 023523. [CrossRef]

44. Solà, J.; Gómez-Valent, A.; de Cruz Pérez, J. The H_0 tension in light of vacuum dynamics in the Universe. *Phys. Lett. B* **2017**, *774*, 317–324. [CrossRef]
45. Nunes, R.C. Structure formation in $f(T)$ gravity and a solution for H_0 tension. *J. Cosmol. Astropart. Phys.* **2018**, *2018*, 052. [CrossRef]
46. Yang, W.; Pan, S.; Di Valentino, E.; Nunes, R.C.; Vagnozzi, S.; Mota, D.F. Tale of stable interacting dark energy, observational signatures, and the H_0 tension. *J. Cosmol. Astropart. Phys.* **2018**, *2018*, 019. [CrossRef]
47. Yang, W.; Mukherjee, A.; Di Valentino, E.; Pan, S. Interacting dark energy with time varying equation of state and the H_0 tension. *Phys. Rev. D* **2018**, *98*, 123527. [CrossRef]
48. Yang, W.; Pan, S.; Di Valentino, E.; Saridakis, E.N.; Chakraborty, S. Observational constraints on one-parameter dynamical dark-energy parametrizations and the H_0 tension. *Phys. Rev. D* **2019**, *99*, 043543. [CrossRef]
49. Poulin, V.; Smith, T.L.; Karwal, T.; Kamionkowski, M. Early dark energy can resolve the Hubble tension. *Phys. Rev. Lett.* **2019**, *122*, 221301. [CrossRef]
50. Mörtsell, E.; Dhawan, S. Does the Hubble constant tension call for new physics? *J. Cosmol. Astropart. Phys.* **2018**, *2018*, 025. [CrossRef]
51. Martinelli, M.; Hogg, N.B.; Peirone, S.; Bruni, M.; Wands, D. Constraints on the interacting vacuum–geodesic CDM scenario. *Mon. Not. R. Astron. Soc.* **2019**, *488*, 3423–3438. [CrossRef]
52. Vattis, K.; Koushiappas, S.M.; Loeb, A. Dark matter decaying in the late Universe can relieve the H_0 tension. *Phys. Rev. D* **2019**, *99*, 121302. [CrossRef]
53. Kumar, S.; Nunes, R.C.; Yadav, S.K. Dark sector interaction: A remedy of the tensions between CMB and LSS data. *Eur. Phys. J. C* **2019**, *79*, 1–5. [CrossRef]
54. Agrawal, P.; Cyr-Racine, F.-Y.; Pinner, D.; Randall, L. Rock'n'Roll Solutions to the Hubble Tension. *arXiv* **2019**, arXiv:1904.01016.
55. Yang, W.; Pan, S.; Di Valentino, E.; Paliathanasis, A.; Lu, J. Challenging bulk viscous unified scenarios with cosmological observations. *Phys. Rev. D* **2019**, *100*, 103518. [CrossRef]
56. Yang, W.; Mena, O.; Pan, S.; Di Valentino, E. Dark sectors with dynamical coupling. *Phys. Rev. D* **2019**, *100*, 083509. [CrossRef]
57. Di Valentino, E.; Ferreira, R.Z.; Visinelli, L.; Danielsson, U. Late time transitions in the quintessence field and the H0 tension. *Phys. Dark Universe* **2019**, *26*, 100385. [CrossRef]
58. Pan, S.; Yang, W.; Di Valentino, E.; Saridakis, E.N.; Chakraborty, S. Interacting scenarios with dynamical dark energy: Observational constraints and alleviation of the H_0 tension. *Phys. Rev. D* **2019**, *100*, 103520. [CrossRef]
59. Martinelli, M.; Tutusaus, I. CMB tensions with low-redshift H_0 and S_8 measurements: Impact of a redshift-dependent type-Ia supernovae intrinsic luminosity. *Symmetry* **2019**, *11*, 986. [CrossRef]
60. Pan, S.; Yang, W.; Di Valentino, E.; Shafieloo, A.; Chakraborty, S. Reconciling H0 tension in a six parameter space? *J. Cosmol. Astropart. Phys.* **2020**, *2020*, 62. [CrossRef]
61. Di Valentino, E.; Melchiorri, A.; Silk, J. Cosmological constraints in extended parameter space from the Planck 2018 Legacy release. *J. Cosmol. Astropart. Phys.* **2020**, *2020*, 013. [CrossRef]
62. Di Valentino, E.; Melchiorri, A.; Mena, O.; Vagnozzi, S. Interacting dark energy in the early 2020s: A promising solution to the H0 and cosmic shear tensions. *Phys. Dark Universe* **2020**, *30*, 100666. [CrossRef]
63. Di Valentino, E.; Melchiorri, A.; Mena, O.; Vagnozzi, S. Nonminimal dark sector physics and cosmological tensions. *Phys. Rev. D* **2020**, *101*, 063502. [CrossRef]
64. Colgain, E.O.; Yavartanoo, H. Testing the Swampland: H_0 tension. *Phys. Lett. B* **2019**, *797*, 134907. [CrossRef]
65. Alcaniz, J.; Bernal, N.; Masiero, A.; Queiroz, F.S. Light dark matter: A common solution to the lithium and H0 problems. *Phys. Lett. B* **2021**, *812*, 136008. [CrossRef]
66. Pan, S.; Yang, W.; Singha, C.; Saridakis, E.N. Observational constraints on sign-changeable interaction models and alleviation of the H_0 tension. *Phys. Rev. D* **2019**, *100*, 083539. [CrossRef]
67. Berghaus, K.V.; Karwal, T. Thermal friction as a solution to the Hubble tension. *Phys. Rev. D* **2020**, *101*, 083537. [CrossRef]
68. Knox, L.; Millea, M. Hubble constant hunter's guide. *Phys. Rev. D* **2020**, *101*, 043533. [CrossRef]
69. Pandey, K.L.; Karwal, T.; Das, S. Alleviating the H_0 and σ_8 anomalies with a decaying dark matter model. *J. Cosmol. Astropart. Phys.* **2020**, *2020*, 026. [CrossRef]
70. Adhikari, S.; Huterer, D. Super-CMB fluctuations and the Hubble tension. *Phys. Dark Universe* **2020**, *28*, 100539. [CrossRef]
71. Hart, L.; Chluba, J. Updated fundamental constant constraints from Planck 2018 data and possible relations to the Hubble tension. *Mon. Not. R. Astron. Soc.* **2020**, *493*, 3255–3263. [CrossRef]
72. Liao, K.; Shafieloo, A.; Keeley, R.E.; Linder, E.V. Determining model-independent H_0 and consistency tests. *Astrophys. J. Lett.* **2020**, *895*, L29. [CrossRef]
73. Benevento, G.; Hu, W.; Raveri, M. Can late dark energy transitions raise the Hubble constant? *Phys. Rev. D* **2020**, *101*, 103517. [CrossRef]
74. Vagnozzi, S. New physics in light of the H_0 tension: An alternative view. *Phys. Rev. D* **2020**, *102*, 023518. [CrossRef]
75. Chudaykin, A.; Gorbunov, D.; Nedelko, N. Combined analysis of Planck and SPTPol data favors the early dark energy models. *J. Cosmol. Astropart. Phys.* **2020**, *2020*, 013. [CrossRef]
76. Alestas, G.; Kazantzidis, L.; Perivolaropoulos, L. H_0 tension, phantom dark energy, and cosmological parameter degeneracies. *Phys. Rev. D* **2020**, *101*, 123516. [CrossRef]

77. Wang, D.; Mota, D. Can $f(T)$ gravity resolve the H_0 tension? *Phys. Rev. D* **2020**, *102*, 063530. [CrossRef]
78. Blinov, N.; Marques-Tavares, G. Interacting radiation after Planck and its implications for the Hubble Tension. *J. Cosmol. Astropart. Phys.* **2020**, *2020*, 029. [CrossRef]
79. Di Valentino, E.; Anchordoqui, L.A.; Ali-Haimoud, Y.; Amendola, L.; Arendse, N.; Asgari, M.; Ballardini, M.; Battistelli, E.; Benetti, M.; Birrer, S. Cosmology intertwined II: The Hubble constant tension. *arXiv* **2020**, arXiv:2008.11284.
80. Di Valentino, E.; Mena, O.; Pan, S.; Visinelli, L.; Yang, W.; Melchiorri, A.; Mota, D.F.; Riess, A.G.; Silk, J. In the Realm of the Hubble tension—A Review of Solutions. *arXiv* **2021**, arXiv:2103.01183.
81. Alestas, G.; Kazantzidis, L.; Perivolaropoulos, L. A $w-M$ phantom transition at $z_t < 0.1$ as a resolution of the Hubble tension. *arXiv* **2020**, arXiv:2012.13932.
82. Camarena, D.; Marra, V. Hockey-stick dark energy is not a solution to the H_0 crisis. *arXiv* **2021**, arXiv:2101.08641 .
83. Sen, A. Deviation from ΛCDM: Pressure parametrization. *Phys. Rev. D* **2008**, *77*, 043508. [CrossRef]
84. Delubac, T.; Bautista, J.E.; Rich, J.; Kirkby, D.; Bailey, S.; Font-Ribera, A.; Slosar, A.; Lee, K.-G.; Pieri, M.M.; Hamilton, J.-C. Baryon acoustic oscillations in the Lyα forest of BOSS DR11 quasars. *Astron. Astrophys.* **2015**, *574*, A59. [CrossRef]
85. Poulin, V.; Boddy, K.K.; Bird, S.; Kamionkowski, M. Implications of an extended dark energy cosmology with massive neutrinos for cosmological tensions. *Phys. Rev. D* **2018**, *97*, 123504. [CrossRef]
86. Aghanim, N.; Akrami, Y.; Ashdown, M.; Aumont, J.; Baccigalupi, C.; Ballardini, M.; Banday, A.J.; Barreiro, R.; Bartolo, N.; Basak, S. Planck 2018 results-V. CMB power spectra and likelihoods. *Astron. Astrophys.* **2020**, *641*, A5.
87. Efstathiou, G.; Gratton, S. A detailed description of the CamSpec likelihood pipeline and a reanalysis of the Planck high frequency maps. **arXiv** *2019*, arXiv:1910.00483 .
88. Beutler, F.; Blake, C.; Colless, M.; Jones, D.H.; Staveley-Smith, L.; Campbell, L.; Parker, Q.; Saunders, W.; Watson, F. The 6dF Galaxy Survey: Baryon acoustic oscillations and the local Hubble constant. *Mon. Not. R. Astron. Soc.* **2011**, *416*, 3017–3032. [CrossRef]
89. Ross, A.J.; Samushia, L.; Howlett, C.; Percival, W.J.; Burden, A.; Manera, M. The clustering of the SDSS DR7 main Galaxy sample–I. A 4 per cent distance measure at $z = 0.15$. *Mon. Not. R. Astron. Soc.* **2015**, *449*, 835–847. [CrossRef]
90. Alam, S.; Ata, M.; Bailey, S.; Beutler, F.; Bizyaev, D.; Blazek, J.A.; Bolton, A.S.; Brownstein, J.R.; Burden, A.; Chuang, C.-H. The clustering of galaxies in the completed SDSS-III Baryon Oscillation Spectroscopic Survey: Cosmological analysis of the DR12 galaxy sample. *Mon. Not. R. Astron. Soc.* **2017**, *470*, 2617–2652. [CrossRef]
91. de Mattia, A.; Ruhlmann-Kleider, V.; Raichoor, A.; Ross, A.J.; Tamone, A.; Zhao, C.; Alam, S.; Avila, S.; Burtin, E.; Bautista, J. The Completed SDSS-IV extended Baryon Oscillation Spectroscopic Survey: Measurement of the BAO and growth rate of structure of the emission line galaxy sample from the anisotropic power spectrum between redshift 0.6 and 1.1. *Mon. Not. R. Astron. Soc.* **2021**, *501*, 5616–5645.
92. Scolnic, D.M.; Jones, D.; Rest, A.; Pan, Y.; Chornock, R.; Foley, R.; Huber, M.; Kessler, R.; Narayan, G.; Riess, A. The complete light-curve sample of spectroscopically confirmed SNe Ia from Pan-STARRS1 and cosmological constraints from the combined pantheon sample. *Astrophys. J.* **2018**, *859*, 101. [CrossRef]
93. Aghanim, N.; Akrami, Y.; Ashdown, M.; Aumont, J.; Baccigalupi, C.; Ballardini, M.; Banday, A.J.; Barreiro, R.; Bartolo, N.; Basak, S. Planck 2018 results-VIII. Gravitational lensing. *Astron. Astrophys.* **2020**, *641*, A8.
94. Lewis, A.; Bridle, S. Cosmological parameters from CMB and other data: A Monte Carlo approach. *Phys. Rev. D* **2002**, *66*, 103511. [CrossRef]
95. Gelman, A.; Rubin, D.B. Inference from iterative simulation using multiple sequences. *Stat. Sci.* **1992**, *7*, 457–472. [CrossRef]
96. Lewis, A. Efficient sampling of fast and slow cosmological parameters. *Phys. Rev. D* **2013**, *87*, 103529. [CrossRef]
97. Asgari, M.; Tröster, T.; Heymans, C.; Hildebrandt, H.; van den Busch, J.L.; Wright, A.H.; Choi, A.; Erben, T.; Joachimi, B.; Joudaki, S. KiDS+ VIKING-450 and DES-Y1 combined: Mitigating baryon feedback uncertainty with COSEBIs. *Astron. Astrophys.* **2020**, *634*, A127. [CrossRef]
98. Zarrouk, P.; Burtin, E.; Gil-Marín, H.; Ross, A.J.; Tojeiro, R.; Pâris, I.; Dawson, K.S.; Myers, A.D.; Percival, W.J.; Chuang, C.-H. The clustering of the SDSS-IV extended Baryon Oscillation Spectroscopic Survey DR14 quasar sample: Measurement of the growth rate of structure from the anisotropic correlation function between redshift 0.8 and 2.2. *Mon. Not. R. Astron. Soc.* **2018**, *477*, 1639–1663. [CrossRef]
99. de Sainte Agathe, V.; Balland, C.; Des Bourboux, H.D.M.; Blomqvist, M.; Guy, J.; Rich, J.; Font-Ribera, A.; Pieri, M.M.; Bautista, J.E.; Dawson, K. Baryon acoustic oscillations at z = 2.34 from the correlations of Lyα absorption in eBOSS DR14. *Astron. Astrophys.* **2019**, *629*, A85. [CrossRef]
100. Blomqvist, M.; Des Bourboux, H.D.M.; de Sainte Agathe, V.; Rich, J.; Balland, C.; Bautista, J.E.; Dawson, K.; Font-Ribera, A.; Guy, J.; Le Goff, J.-M. Baryon acoustic oscillations from the cross-correlation of Lyα absorption and quasars in eBOSS DR14. *Astron. Astrophys.* **2019**, *629*, A86. [CrossRef]
101. Heavens, A.; Fantaye, Y.; Sellentin, E.; Eggers, H.; Hosenie, Z.; Kroon, S.; Mootoovaloo, A. No evidence for extensions to the standard cosmological model. *Phys. Rev. Lett.* **2017**, *119*, 101301. [CrossRef] [PubMed]
102. Heavens, A.; Fantaye, Y.; Mootoovaloo, A.; Eggers, H.; Hosenie, Z.; Kroon, S.; Sellentin, E. Marginal Likelihoods from Monte Carlo Markov Chains. *arXiv* **2017**, arXiv:1704.03472 .
103. Kass, R.; Raftery, A. Bayes factor and model uncertainty. *J. Am. Stat. Assoc.* **1995**, *90*, 773–795. [CrossRef]